PHOTOMASK

BACUS—The international technical group of SPIE dedicated to the advancement of photomask technology.

BACUS N • E • W • S

MARCH 2021
VOLUME 37, ISSUE 3

EUVL20 - Invited Paper

Mask absorber for next generation EUV lithography

Meiyi Wu and Devesh Thakare, imec, Kapeldreef 75, B-3001 Leuven, Belgium; KU Leuven Department of Chemistry, Leuven, Belgium

Jean-François de Marneffe, Patrick Jaenen, Laurent Souriau, Karl Opsomer, Jean-Philippe Soulié, and Vicky Philipsen, imec, Kapeldreef 75, B-3001 Leuven, Belgium

Andreas Erdmann and Hazem Mesilhy, Fraunhofer Institute for Integrated Systems and Device Technology, Schottkystrasse 10, 91058 Erlangen, Germany

Philipp Naujok, optiX fab GmbH, Hans-Knoell-Strasse 6, 07745 Jena, Germany

Markus Foltin, Süss MicroTec Photomask Equipment GmbH & Co. KG, Ferdinand-von-Steinbeis-Ring 10, 75447 Sternenfels, Germany

Victor Soltwisch and Qais Saadeh, Physikalisch-Technische Bundesanstalt, Abbestr. 2-12, 10587 Berlin, Germany

ABSTRACT

Novel mask absorber designs are calling attention of the EUVL community due to their ability to mitigate mask 3D effects. Material selection is part of such optimization[1]. In this paper we propose several candidates as novel EUV lithography mask absorbers, namely TaTeN, Ru-Ta and Pt-Mo alloys.

The choice of these materials is based on their theoretical performance evaluated by EUV imaging simulation based on their complex refractive index N(λ) = n(λ) +ik(λ), where the optical constants n and k relate to the phase velocity and to the absorption of an electromagnetic radiation with a wavelength λ, respectively. The materials are deposited as thin films on Si substrate with an additional Ru layer to mimic the cap of multilayer mirror (MLM) on the real mask. The experimental n & k values are determined by analyzing EUV reflectivity data obtained using a 13.5 nm synchrotron EUV radiation. The imaging simulation presented in this paper consists of calculation of several imaging metrics like non-telecentricity, normalized image log-slop (NILS), and threshold-to-size for specific use cases using the novel absorber. It also compares the proposed materials to the reference TaBN absorber. TaTeN shows higher absorption than TaBN and refraction closer

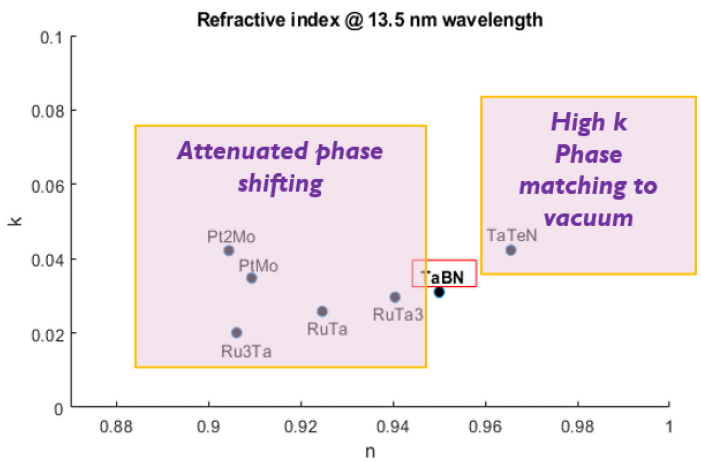

Figure 1. Complex refractive index of binary alloy materials determined by EUVR analysis.

TAKE A LOOK INSIDE:

INDUSTRY BRIEFS
—see page 12

CALENDAR
For a list of meetings
—see page 13

SPIE.

11517-2

Editorial

Let's do our small part to make the world a better place.

Kent Nakagawa, Toppan Photomasks, Inc.

Bear with me, as this editorial starts off with another "pandemic" theme. I assure you that it is much more than that.

In the recent past, this month would be the heart of my winter conference travel season. In fact, last year I was wrapping up what turned out to be my last live conference trip just as the world began to shut down due to COVID-19. You know the rest of the tale – quarantines and social distancing. Work from home. Virtual conferences and meetings. And it continues this year, with my normal travel routine taking a back seat for at least another 6 months (or longer).

We have also born witness to the tools that have enabled this virtualization change. Our semiconductor industry has been the enabler to make cloud computing, home-to-work networking, virtual office visits, and the like, possible. Although we have had our own disruptions on how to manage employee interactions, as a business, we have been least negatively impacted by the pandemic, and in some respects, we may actually have been one of the few beneficiaries of the resulting product demands.

However, it was not too far removed from my "normal travel routine" to see the huge negative fallout. The collapse of the service industries that I relied on – airlines, hotels, restaurants – and the unemployment of these people that I would engage with on my travels. And over the course of the year, as I see the forced shift to online education, virtual doctor visits, and e-commerce as examples, I am very much aware of the increasing divide in our populations over fundamental access to these new modes of learning, shopping, healthcare, etc.

It's the same with access to information. The internet is a two-edged sword, both in terms of access to information, but also dissemination of credible and misleading or false information. For those who have access, there's literally too much information that can be gathered without a way to easily identify the quality of information. Worse – our ability to critically assess information has been replaced by simple browser searches, or posts on social media and blogs. And those who have no access to technology are forced to rely on word-of-mouth…even further away in context from the actual facts and background information. The two dominant news events in the US this year – pandemic response and the US election season – are a clear testament to just how easy it is to present two polar opposite narratives as truth. And our technology plays an enabling role in this.

We have the privilege of enabling and building tools to advance our technology and our society. But we should also have an obligation to help our society make use of our technology in a helpful, not harmful, manner. As engineers and scientists, it is critical that we help people learn how to make use of the information that is now readily available –to interpret, critique, and understand information, discern facts from deception, and perhaps "humanize" our technological advancements. Ultimately, we are some of the best equipped persons to bridge the gap between technology and the masses. One person at a time. One group at a time.

BACUS N • E • W • S

BACUS News is published monthly by SPIE for *BACUS*, the international technical group of SPIE dedicated to the advancement of photomask technology.

Managing Editor/Graphics Linda DeLano

SPIE Sales Representative, Exhibitions, and Sponsorships Melissa Valum

BACUS Technical Group Manager Tim Lamkins

SPIE.

P.O. Box 10, Bellingham, WA 98227-0010 USA
Tel: +1 360 676 3290
Fax: +1 360 647 1445
SPIE.org
help@spie.org

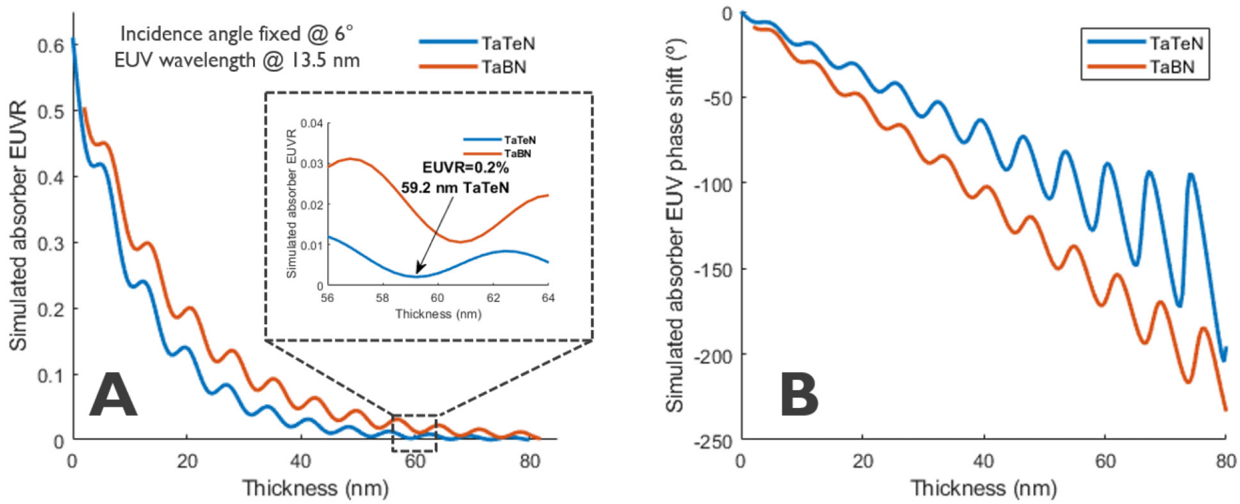

Figure 2. Simulation of EUVR (A) and EUV phase shift (B) of TaTeN and TaBN absorber as function of absorber thickness. EUVR between 56 and 60 nm is zoomed to highlight the optimum TaTeN thickness of 59.2 nm which gives reduced EUVR of 0.2%.

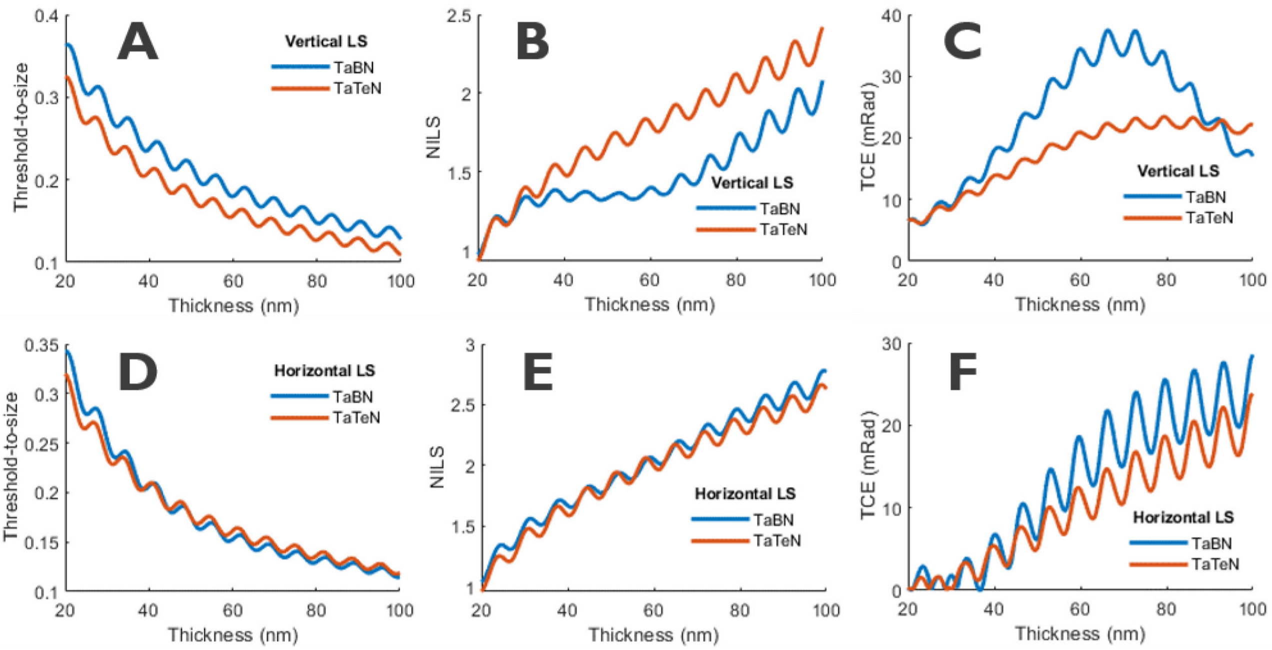

Figure 3. Simulation of EUV imaging performance as function of absorber thickness with TaTeN and TaBN. Vertical LS feature: T2S (A), NILS (B) and TCE (C). Horizontal LS feature: T2S (D), NILS (E) and TCE (F).

to 1, which improves phase matching for a high k absorber. The refractive index of Ru-Ta and Pt-Mo alloys exhibits a large difference to that of air and provides the required phased shift of attenuated phase shift masks[2].

The characterizations of these materials target the requirements of an EUVL mask: durability for mask cleaning, mask lifetime and etchablity for mask patterning. The stability is first tested against several standard mask cleaning solutions by beaker test up to 24 hours with the film structure monitored by X-ray reflectivity analysis. The samples are also exposed to hydrogen plasma to imitate the working environment in a EUV scanner. Material integrity is checked with Rutherford backscattering spectroscopy before and after the exposure. Concerning material patterning, chemical reactive ion etch is applied for preliminary tests. A proper etch recipe is found for TaTeN with good etch rate (about 60 nm/min) and good selectivity to Ru underlayer (Ru etch is ignorable).

Introduction

The mask-induced imaging effects in EUV lithography can be mitigated by modifying the design of EUV mask. Such modification can be multilayer (ML) optimization not only to increase the EUV reflectivity, but also to obtain a certain angular response of the multilayer and to reduce the distance between the effective reflectivity plane and the multilayer surface[3]. This includes fine tuning of multilayer period[4], replacing the

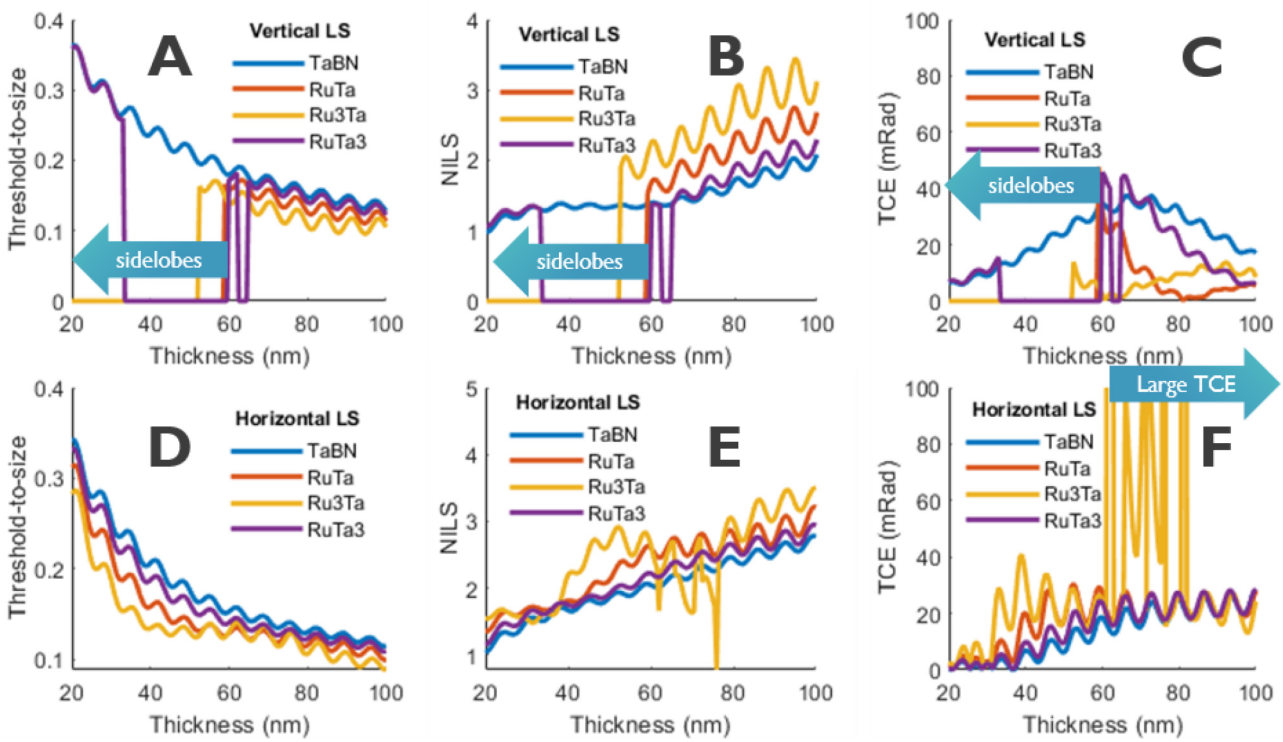

Figure 4. Simulation of EUV imaging performance as function of absorber thickness with Ru-Ta alloys and TaBN. Vertical LS feature: T2S (A), NILS (B) and TCE (C). Horizontal LS feature: T2S (D), NILS (E) and TCE (F).

material Mo/Si[5] and patterning of the multilayer[6]. Another solution is the absorber optimization. Tuning the current state-of-art TaBN absorber is one of the options. But previous study shows that TaBN is at its limit for imaging extendibility[7].

Alternatively, novel mask absorber material is a more realistic approach[8] to either increase the EUV absorption or, in the case of attenuated phase shift mask (attPSM), to enhance EUV refraction. As single metal absorbers are reported suffering from full-layer crystallization[9], binary alloys bring the advantage of tuning the properties, not only in terms of optical constants, but also in term of material morphology and stability[10]. In this paper, we propose several binary alloys to replace TaBN as EUV mask absorber.

Material Selection

The material selection of EUV absorber candidates is based on the material optical constant n & k map for EUVL imaging improvement expectation reported by Philipsen[1]. Single elements, namely Ru, Pt and Te, are selected for their theoretically favorable EUV properties compared to the starting point TaBN. Te has higher extinction coefficient k than TaBN, which may help reduce the absorber thickness and as a result, smaller shadowing effect thanks to its increased EUV absorption.

It also has refraction coefficient n closer to that of vacuum, reducing phase deformation. Ru and Pt possess refraction coefficient lower than TaBN and away from that of vacuum, leading to enhanced phase shift character for which higher imaging contrast can be expected. However, as mentioned in introduction, single metal absorber might exhibit disadvantages, such as the instability of Te single metal[10]. Selecting Ta (which is a known stable absorber material) as a starting point, several alloys are proposed, namely TaTe, Ru_3Ta, RuTa, $RuTa_3$. Particularly for TaTe, N doping is considered with the purpose of reducing oxidation and crystallinity. Pt_2Mo, PtMo are also proposed although their stabilities remain unknow. We will explore that in later section of this paper.

For these absorber candidates, optical constants are experimentally determined by EUV reflectivity (EUVR) analysis conducted in PTB[11]. Using reflectivity data collected in the PTB Soft X-ray laboratory in the electron storage ring facility BESSY II, the optical constants are reconstructed by optimizing an inverse problem using the Differential Evolution algorithm[12], this approach is well suited for characterization of the probed thin films where no sample preparation is required as it allows the simultaneous reconstruction of the two components of the complex refractive index at a wavelength of 13.5 nm. The result is presented in Figure 1. TaTeN exhibits better EUV absorption and less phase variation compared to TaBN, while Ru-Ta and Pt-Mo alloys make a fine match as absorber material for attenuated phase shift mask. The advantage of optical constant tuning by using alloy material is well shown. For example, one may easily find that by changing Ru:Ta ratio, Ru-Ta alloys cover a wide range on the n&k map.

Simulation

The simulations presented in this paper are performed with the experimentally determined optical constants n & k of the materials in Figure 1. We start the study by simulation of mask EUVR and EUV phase shift at 13.5 nm wavelength while varying the absorber thickness. The normal incidence angle of the EUV beam is fixed at 6° to mimic the imaging condition in EUV scanner. A Mo/Si multilayer is placed under the absorber to complete the mask blanket design[13]. For the same absorber thickness, TaTeN can always provide lower reflection (Figure 2 A), thus better absorption compared to TaBN. The optimum thicknesses of TaTeN can be taken at troughs of the oscillating EUVR curve: 38.4 nm, 45.2 nm, 52.4 nm, and 59.2 nm. Particularly, with a 59.2 nm TaTeN absorber, an EUVR of 0.2% can be achieved, which is much lower than the 1% EUVR of a TaBN absorber with optimum thickness around 60 nm. Other than that, TaTeN also shows less EUV phase shift (Figure 2 B), which should bring gain in lowering the telecentricity error.

The EUV imaging simulation compared to the TaBN while varying the absorber thickness is presented in Figure 3. Considered imaging metrics include threshold to size (T2S), normalized image log-slope (NILS) and telecentricity error (TCE). As our absorbers are meant for the next generation EUVL, we use numerical aperture (NA) of 0.55 with the use case of pitch 32 nm equal line space (LS) and small leaf dipole illumination.

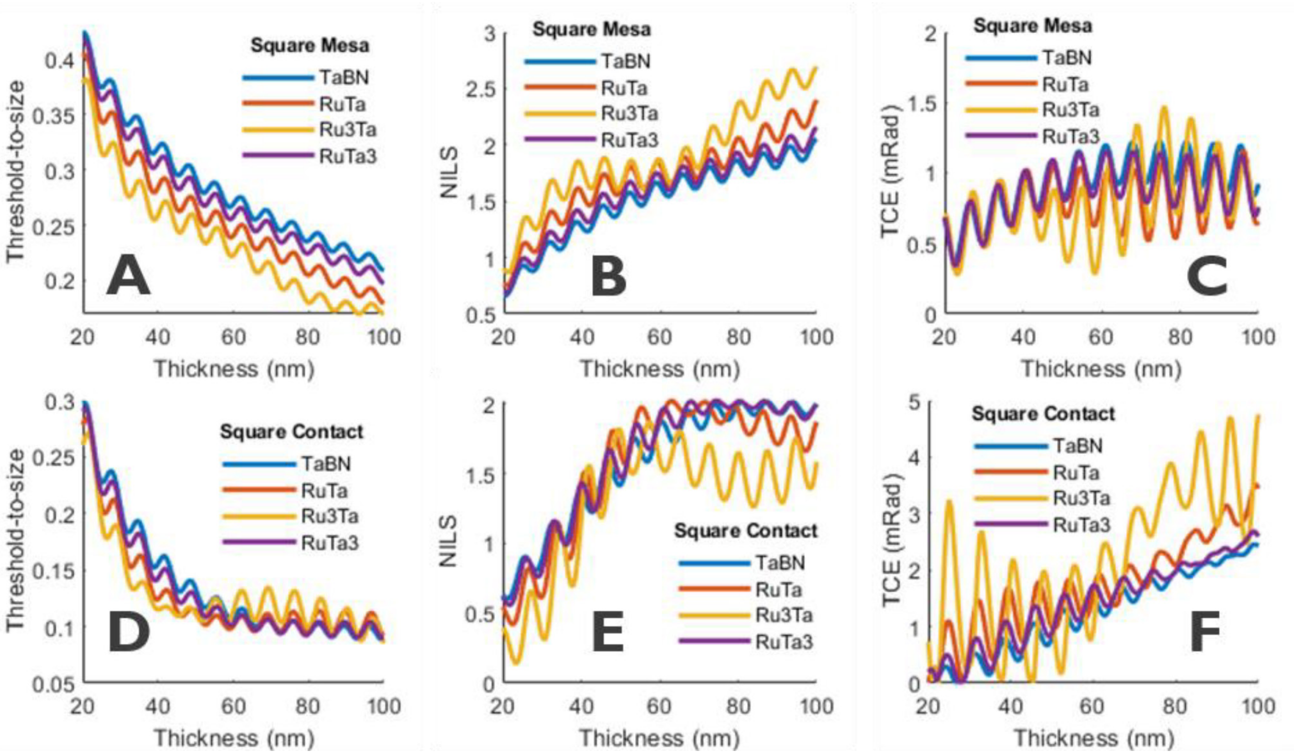

Figure 5. Simulation of EUV imaging performance as function of absorber thickness with Ru-Ta alloys and TaBN. Square mesa feature: T2S (A), NILS (B) and TCE (C). Square contact feature: T2S (D), NILS (E) and TCE (F).

Vertical feature is simulated at slit edge while horizontal feature is simulated at slit centre. More details can be found in the paper of Erdmann[14].

For vertical LS feature, TaTeN can provide significantly higher NILS (Figure 3 B) and lower TCE (Figure 3 C) compared to TaBN. This is paid by lower T2S (Figure 3 A). For horizontal LS feature, TaTeN can provide lower TCE (Figure 3 F) while maintaining T2S and NILS (Figure 3 D and E).

Same use case is applied for simulations of EUV imaging metrics for Ru-Ta alloys. The result indicates that Ru-Ta needs careful optimization as a solution for through pitch trenches, see Figure 4.

Below 60 nm thickness of the absorber, the imaging suffers from disrupt jumps, especially for vertical features. These disrupt jumps in the simulated data at certain thickness values result from pronounced sidelobes or from significant shifts of the image position beyond the borders of the metrology window. Above 60 nm, the imaging suffers from low threshold to size. And particularly for horizontal features it has large telecentricity errors.

However, Ru-Ta can be good solution for Mesa and contact as presented in Figure 5. We take a use case of pitch 28 nm target CD 12 nm mesa/contact with quasar illumination[14]. For mesa, Ru-Ta alloys provide significant NILS improvement (Figure 5 B). Such improvement depends not only on the absorber thickness but also on Ru:Ta ratio. Higher NILS is obtained with higher Ru content in the alloy. For contacts, absorber thickness must be carefully tuned in order to gain NILS improvement (Figure 5 E). Telecentricity error is not (very) critical for (dense) mesas/contacts. Low threshold-to-size can be addressed by optical proximity correction (OPC).

For the EUV imaging simulation of Pt-Mo alloys compared to TaBN, again we use the same use case presented earlier for TaTeN and RuTa. The result shows that both compositions, Pt_2Mo and PtMo, can provide significantly higher NILS (Figure 6 B and E), to be paid by lower T2S (Figure 6 A and D) and larger TCE (Figure 6 C and F). However, for larger absorber thickness, Pt-Mo alloys might provide lower TCE, especially for vertical features (Figure 6 C). The abrupt jumps of simulated data result from sidelobes or image position shift, same as explained for the simulation of Ru-Ta alloys in Figure 4.

Pt-Mo alloys can also be good solution as EUV absorber for square mesa and contact features, providing higher NILS than TaBN (Figure 7 B and E), to be paid by lower T2S (Figure 7 A and D).

Such low threshold-to-size can be addressed by OPC. Although telecentricity error is not (very) critical for (dense) mesas/contacts, for Square mesa, Pt-Mo exhibit lower TCE compared to TaBN (Figure 7 C).

Experimental Characterization

The characterization of the absorber material candidates starts with chemical stability assessment by simple beaker tests of TaTeN and Pt-Mo alloys. Coupons of absorber thin film are separately submerged in typical mask cleaning solutions, including deionized water (DIW) and two basic solutions for 24 hours. An additional pristine sample is kept in ambient environment as reference.

After the chemical treatment, all samples are rinsed with deionized water, dried by extreme clean dried air (XCDA). The structures of the absorber thin films are checked with X-ray reflectivity (XRR) analysis using Cu Kα X-ray. The results are then compared to the XRR measurements of the reference samples, as presented in Figure 8. Despite using different angular range setting (0-3° for TaTeN and 0-2° for Pt-Mo alloys), the feature of the XRR curves exhibit similar properties, which is a good indication that the structures of the absorber thin films remain the same after the beaker test.

Specifically, for each material, the location of critical angle of the XRR curves remain the same, which means the bulk density of the film is not changed. Also, the frequency of the curve oscillation remains the same which mean the total thickness is not changed (only minor variation due to the fact that the coupons have initial difference in thickness among them).

For Ru-Ta, chemical stability is also assessed particularly for RuTa for its standing out morphology property, which is discussed elsewhere[15]. The beaker tests provide qualitative tendencies to check material dissolvability for RuTa coupons in a variety of wet acidic, alkaline and/or oxidizing standard cleaning media. 6 coupons are prepared for these tests, in which 1 serves as reference and the other 5 are immersed for 24 hours in separated beakers filled with all types of cleaning liquids.

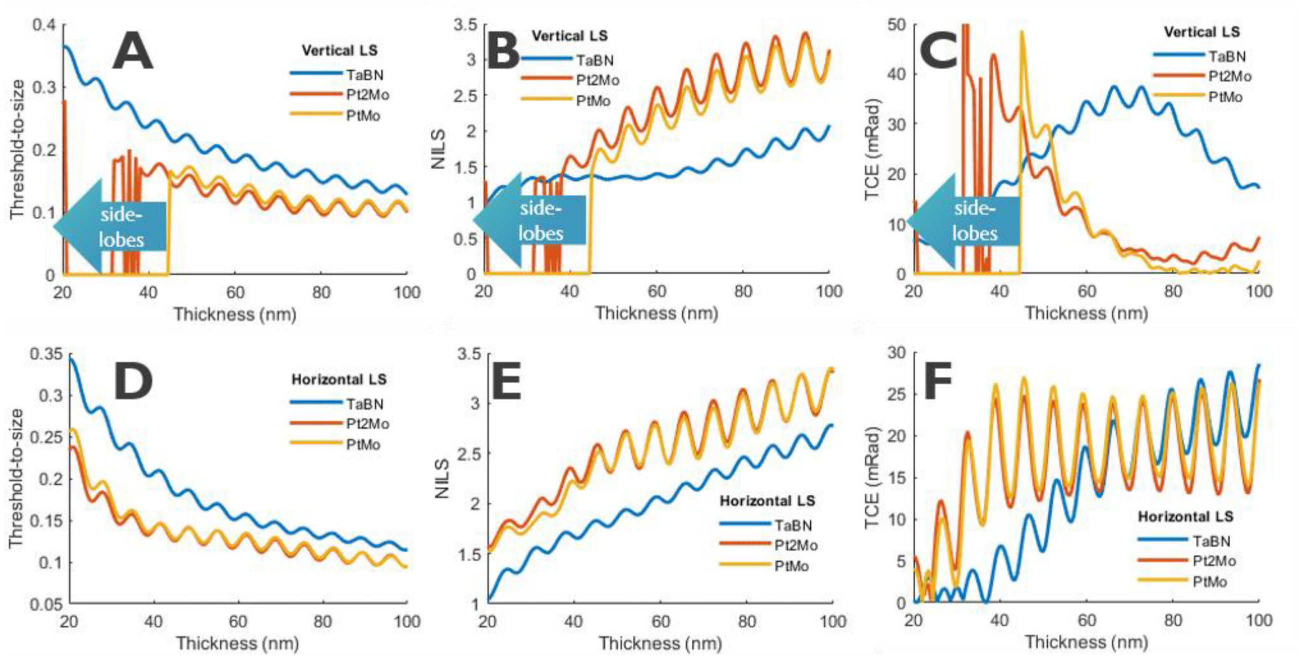

Figure 6. Simulation of EUV imaging performance as function of absorber thickness with Pt-Mo alloys and TaBN. Vertical LS feature: T2S (A), NILS (B) and TCE (C). Horizontal LS feature: T2S (D), NILS (E) and TCE (F).

XRR inspection result is presented in Figure 9. In these preliminary tests all RuTa samples show promising chemical inertness in all types of cleaning solutions. The critical angle and primary oscillation of the XRR curves are unchanged, which means the total thickness of bulk material is unchanged and optical constants remain the same. However, the secondary oscillation variation may be related to some surface effects like oxidation.

Industry-oriented mask cleaning test is performed for one RuTa coated wafer blank. The wafer is processed by one automated standard cleaning cycle to verify the preliminary result under regular cleaning conditions. Apart from the cleaning chemistry, the wafer sample is also treated by physical force applications, which could not be investigated in the beaker tests. The processed RuTa coated wafer is inspected by XRR and atomic force microscopy (AFM), in which the structural integrity and surface roughness are evaluated, as presented in Figure 10. Similar to the beaker tests, the material density and optical constants remain unchanged, as can be read from the overlapping critical angle of the two XRR curves. Surface effect can be seen from the secondary oscillation, despite that the total thickness (related to the primary oscillation) remains almost the same before and after the cleaning process. Additionally, the surface roughness before and after the cleaning cycle appears to be very low according to AFM observation.

The materials are then exposed in hydrogen plasma, which is to mimic the hydrogen flow presented in EUV scanners. This is of course not exactly the scanner condition. Although EUV light is unavailable in our test, the hydrogen plasma condition is intentionally set to be more severe than scanner condition. It would bring us information as a first step. This time, after 24h, unfortunately, we observe with Rutherford back scattering spectroscopy (RBS) a huge loss of Te in TaTeN coupon after the exposure, as shown in Figure 11 (left). This instability can be solved by depositing a 5 nm TaN as capping layer. Te loss is not observed any more with the protection of the cap, as can be seen in Figure 11 (right). The Ta and Te content increase from non-capped sample to capped sample is because of the initial difference in thickness of the pristine coupons.

Same test is done for Ru-Ta and Pt-Mo alloys. The results are presented in Figure 12 and Figure 13, respectively. For these materials, the bulk composition is stable in H plasma according to RBS, showing no variation of element content before and after the exposure.

Absorber Patterning

The patterning of the TaTeN is realized by the combination of 193 immersion DUV lithography and reactive ion etch (RIE). Line-space feature pitch 300 nm is patterned for a thin film deposited on a very thin Ru underlayer on Si substrate. The Ru underlayer mimics the capping layer of the multilayer mirror on a EUV mask. Chlorine-based RIE is performed, but residue of the photoresist is observed by cross-section scanning electron microscopy (XSEM) as can be seen in Figure 14 A and B. This is due to the re-sputtering of the alloy onto the resist sidewall. And such residue cannot be stripped with standard method. To solve this problem, we deposit a SiO_2 hardmask (HM) on the TaTeN film before the lithography exposure. The residue problem is well solved. On XSEM Figure 14 C and D, we can see that the hardmask is not consumed, the sidewall is rather straight, the etch stops well at Ru layer, and most importantly there is no more residue.

Next step is to find a way to remove the hardmask without damaging the TaTeN film. As hydrogen fluoride (HF) is known to be able to etch SiO_2, patterned coupons are dipped in HF aqueous solution and eventually a recipe is found to remove SiO_2 while keeping absorber intact. XSEM images in Figure 15 shows that after 30s dip the HM is partially removed, while after 1 min it is entirely removed and TaTeN is not damaged. One must understand that TaTeN does not have a good resistance to HF. The explanation for the observation is that HF has the selectivity to react first with SiO_2. This also means that time is critical for this process as TaTeN loss is expected if the dip is extended.

For RuTa, RIE is performed on blanket film using pure Cl_2 plasma. Two recipes are applied for this process, one with low voltage (LV) and the other with high voltage (HV). The blanket films of RuTa is evaluated by X-ray reflectivity analysis before and after the etch process to get the etched depth.

Etch rate is then easily obtained while considering the time of the etching. It is also mandatory that the etch of RuTa is selective to Ru as Ru is the capping layer of the multilayer mirror under the absorber. Therefore, same process and analysis are done for Ru. The result is presented in Figure 16, where the etch rates of RuTa and Ru are compared. RuTa etch rate is low even with high voltage chlorine plasma, only about 7 nm/min. The RuTa etch selectivity to Ru is achieved about 2.4:1 with LV plasma. As the alloy itself contains Ru, to improve etch selectivity, one may consider

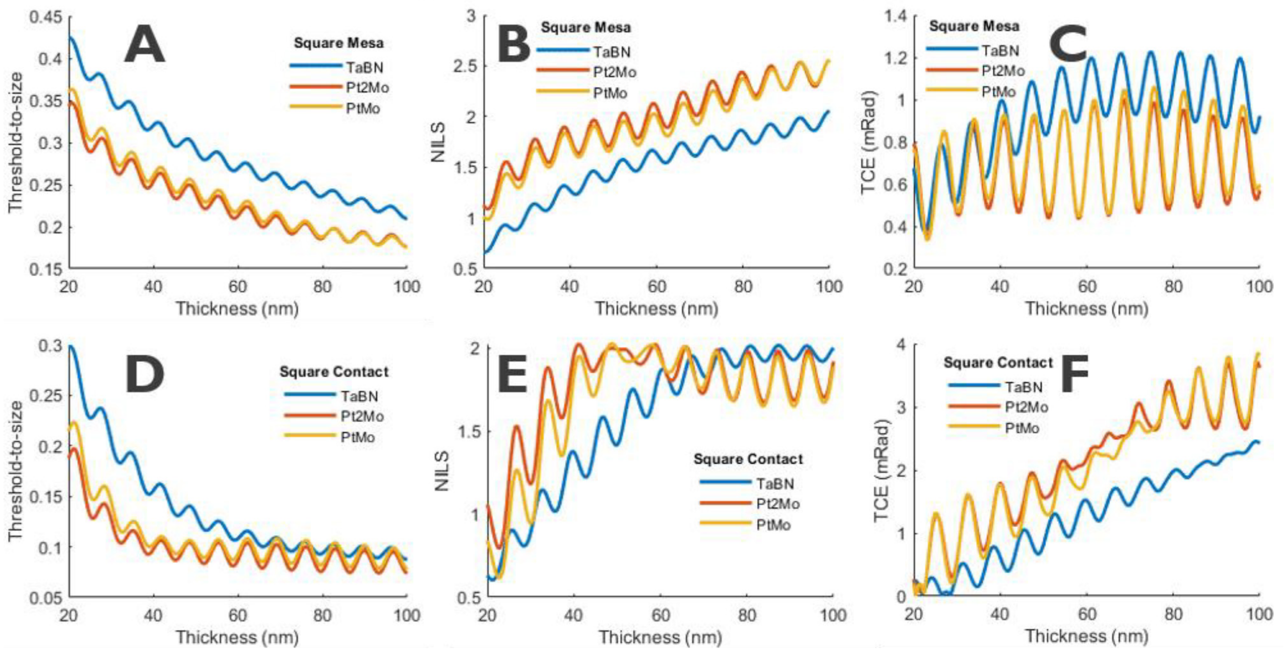

Figure 7. Simulation of EUV imaging performance as function of absorber thickness with Pt-Mo alloys and TaBN. Square mesa feature: T2S (A), NILS (B) and TCE (C). Square contact feature: T2S (D), NILS (E) and TCE (F).

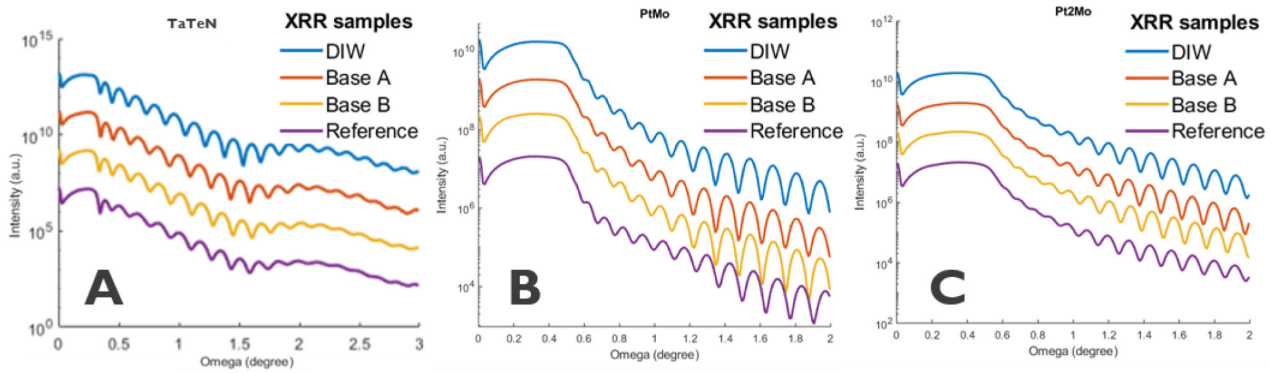

Figure 8. XRR measurements of the beaker tests as well as the reference samples of the absorber materials. A: TaTeN, B: PtMo, C: Pt_2Mo.

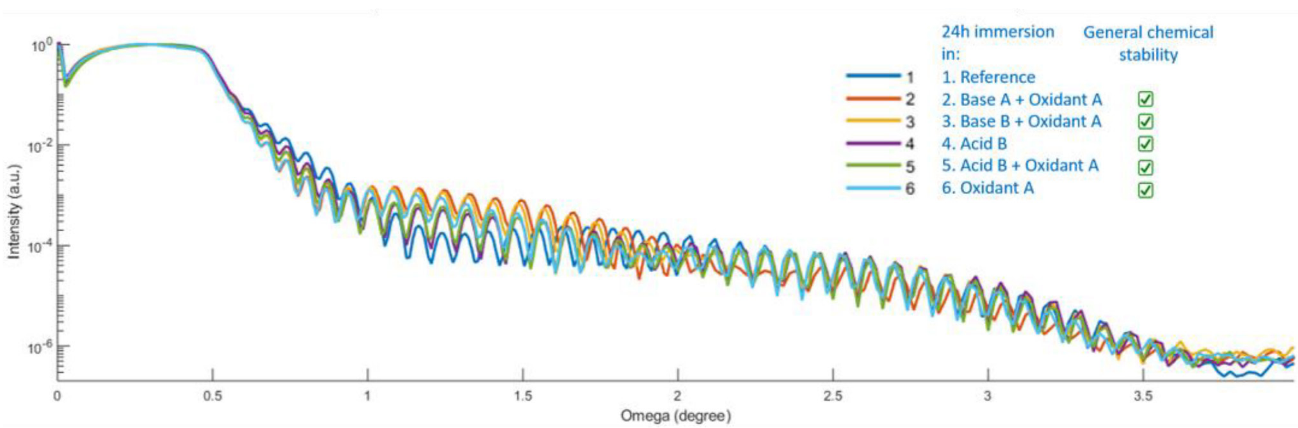

Figure 9. XRR measurements for samples after 24h immersion in acidic, alkaline and/or oxidizing liquids.

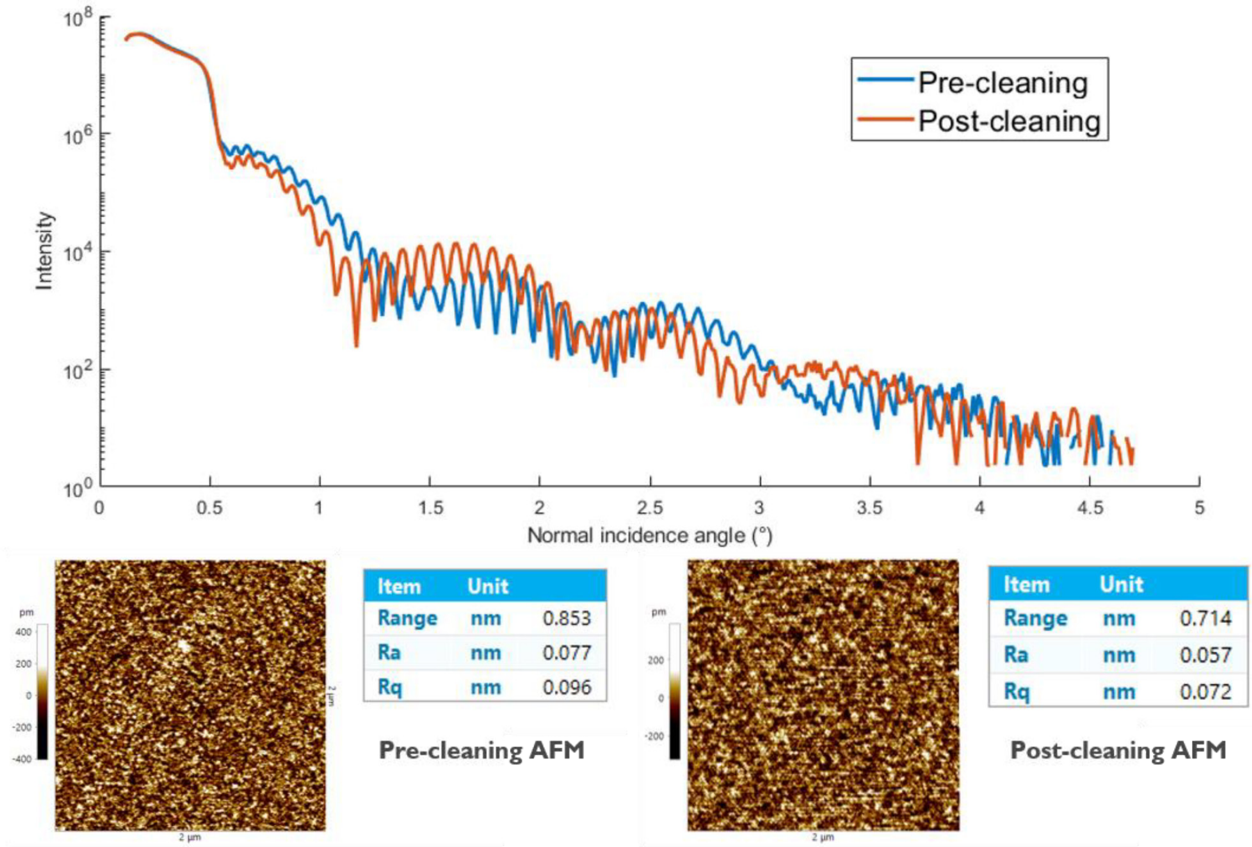

Figure 10. XRR (top) and AFM (bottom) measurements for RuTa coated wafer before and after the cleaning process.

replacing the Ru MLM capping layer with other material. But of course, that would require more dedicated study. The patterning attempt of Pt-Mo alloys is currently ongoing and is not discussed in this paper.

Conclusion

As a conclusion, all 3 candidates show promising properties. The gain in EUV performance is proven by simulation based on experimentally determined optical constants. High k absorber TaTeN provides EUVR lower than TaBN as well as better phase matching to vacuum. EUV imaging simulation shows NILS and TCE improvement for line/space feature. For attenuated phase shift materials Ru-Ta and Pt-Mo alloys, NILS improvement can be expected for contact and mesa designs, although thickness of the absorber must be carefully optimized. Particularly for Pt-Mo alloys, which are high k phase shifting materials, NILS improvement can also be achieved for line/space feature. Spotted minor issues can be solved by process optimization. For example, the TaN capping layer to improve TaTeN stability in hydrogen environment, and the SiO_2 hardmask to prevent photoresist residues during TaTeN etching.

For the future, deposition and patterning of the absorbers on multilayer mirror is planned. With the absorber pattern on multilayer mirror, it is possible to experimentally evaluate the EUV performance such as diffraction quality. But eventually it takes a real mask with novel absorber for EUV printing on imec's EUV scanner to experimentally verify the gain in EUV imaging metrics.

Acknowledgement

The authors acknowledge that this project has received funding from the Electronic Component Systems for European Leadership Joint Undertaking under grant agreement No 783247 - TAPES3. This Joint Undertaking receives support from the European Union's Horizon 2020 research and innovation program alongside Netherlands, France, Belgium, Germany, Czech Republic, Austria, Hungary and Israel.

We appreciate the XSEM support of D. Goossens (imec).

References

[1] V. Philipsen *et al.*, "Mask absorber development to enable next-generation EUVL," in Photomask Japan 2019: XXVI Symposium on Photomask and Next-Generation Lithography Mask Technology, Yokohama, Japan, Jun. 2019, p. 24, doi: 10.1117/12.2537967.

[2] A. Erdmann *et al.*, "Perspectives and tradeoffs of novel absorber materials for high NA EUV lithography (Conference Presentation)", **Proc. SPIE 11323**, Extreme Ultraviolet (EUV) Lithography XI, 1132309 (24 March 2020); https://doi.org/10.1117/12.2550882.

[3] H. M. S. Mesilhy, P. Evanschitzky, G. Bottiglieri, E. van Setten, T. Fliervoet, and A. Erdmann, "Pathfinding the perfect EUV mask: the role of the multilayer," in Extreme Ultraviolet (EUV) Lithography XI, San Jose, United States, Mar. 2020, p. 37, doi: 10.1117/12.2551870.

[4] V. Philipsen *et al.*, "Imaging impact of multilayer tuning in EUV masks, experimental validation," Monterey, California, United States, Oct. 2014, p. 92350J, doi: 10.1117/12.2066222.

[5] O. Wood *et al.*, "Improved Ru/Si multilayer reflective coatings for advanced extreme-ultraviolet lithography photomasks," San Jose, California, United States, Mar. 2016, p. 977619, doi: 10.1117/12.2219215.

[6] A. Erdmann, T. Fuehner, P. Evanschitzky, J. T. Neumann, J. Ruoff, and P. Graeupner, "Modeling studies on alternative EUV mask concepts for higher NA," San Jose, California, USA, Apr. 2013, p. 86791Q, doi: 10.1117/12.2011432.

[7] N. Davydova *et al.*, "Experimental approach to EUV imaging enhancement by mask absorber height optimization," Dresden, Germany, Oct. 2013, p. 88860A, doi: 10.1117/12.2030806.

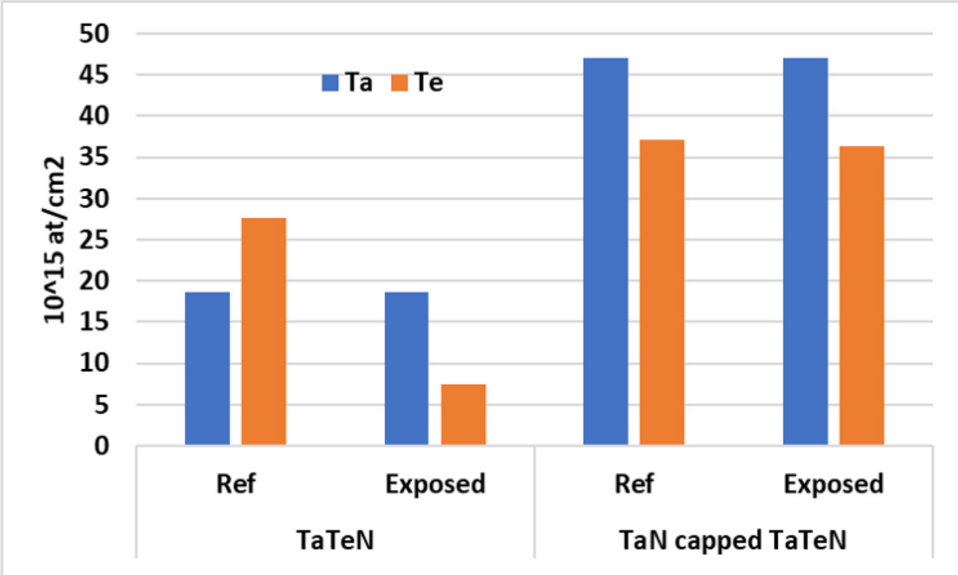

Figure 11. RBS analysis of chemical content of Ta and Te before and after the exposure in H plasma. ***Left:*** *experiment on TaTeN thin film,* ***Right****: experiment on TaTeN thin film with a TaN capping layer.*

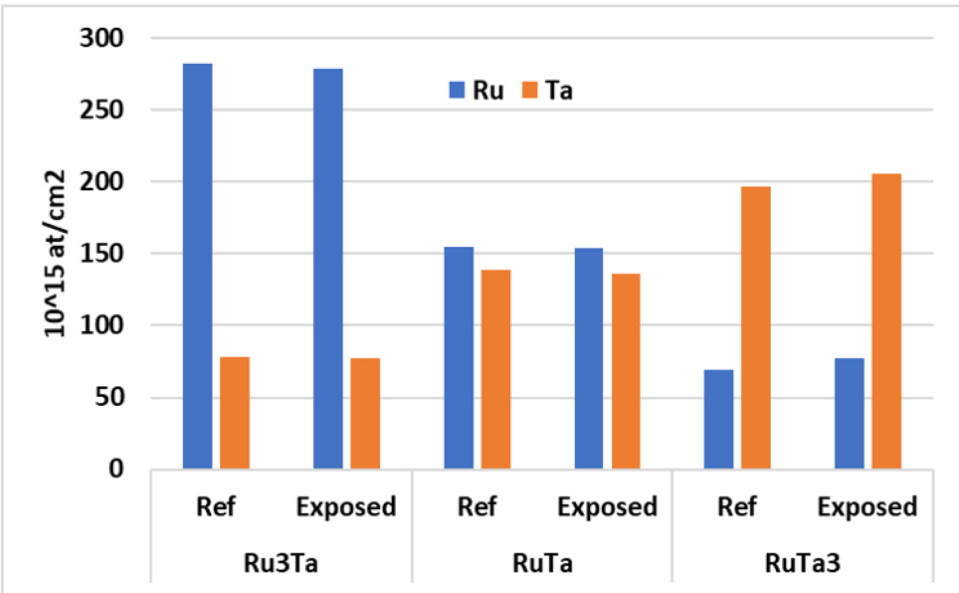

Figure 12. RBS analysis of chemical content of Ru and Ta before and after the exposure in H plasma for Ru-Ta alloys.

[8] V. Philipsen *et al*., "Reducing extreme ultraviolet mask three-dimensional effects by alternative metal absorbers," *Journal of Micro/ Nanolithography, MEMS, and MOEMS,* vol. 16, no. 4, p. 041002, Aug. 2017, doi: 10.1117/1.JMM.16.4.041002.

[9] C. Detavernier *et al*., "Novel EUV mask absorber evaluation in support of next-generation EUV imaging," in Photomask Technology 2018, Monterey, United States, Oct. 2018, p. 11, doi: 10.1117/12.2501799.

[10] V. Luong *et al*., "Assessing stability of metal tellurides as alternative photomask materials for extreme ultraviolet lithography," *Journal of Vacuum Science & Technology B*, vol. 37, no. 6, p. 061607, Nov. 2019, doi: 10.1116/1.5125662.

[11] C. Laubis, K. Vu Luong, V. Philipsen, and F. Scholze, "Update on optical material properties for alternative EUV mask absorber materials," in 33rd European Mask and Lithography Conference, Dresden, Germany, Sep. 2017, p. 16, doi: 10.1117/12.2279702.

[12] R. Storn and K. Price, "Differential Evolution – A Simple and Efficient Heuristic for global Optimization over Continuous Spaces.," *Journal of Global Optimization*, vol. 11, no. 4, pp. 341–359, 1997, doi: 10.1023/A:1008202821328.

[13] V. Philipsen, E. Hendrickx, R. Jonckheere, N. Davydova, T. Fliervoet, and J. T. Neumann, "Actinic characterization and modeling of the EUV mask stack," Dresden, Germany, Oct. 2013, p. 88860B, doi: 10.1117/12.2030663.

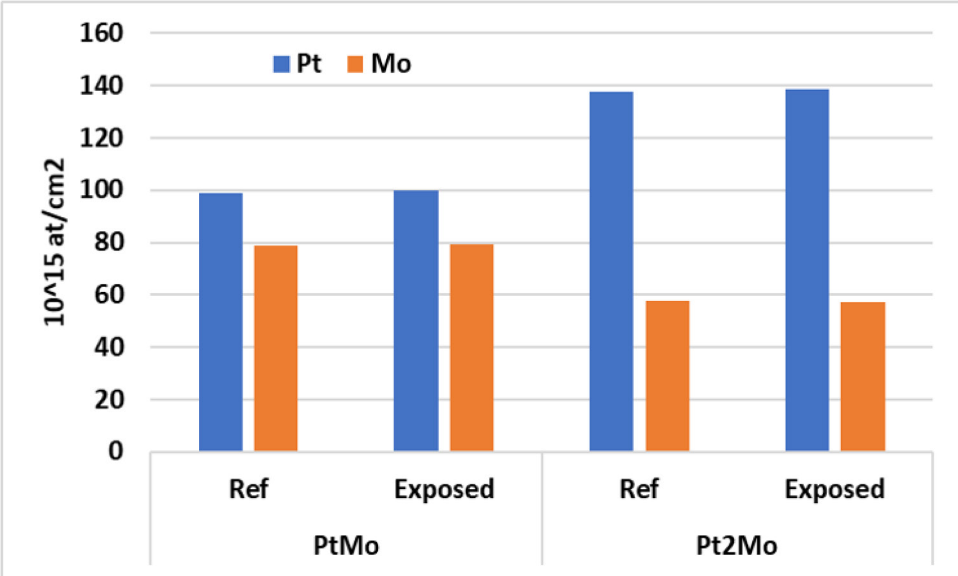

Figure 13. RBS analysis of chemical content of Pt and Mo before and after the exposure in H plasma for Pt-Mo alloys.

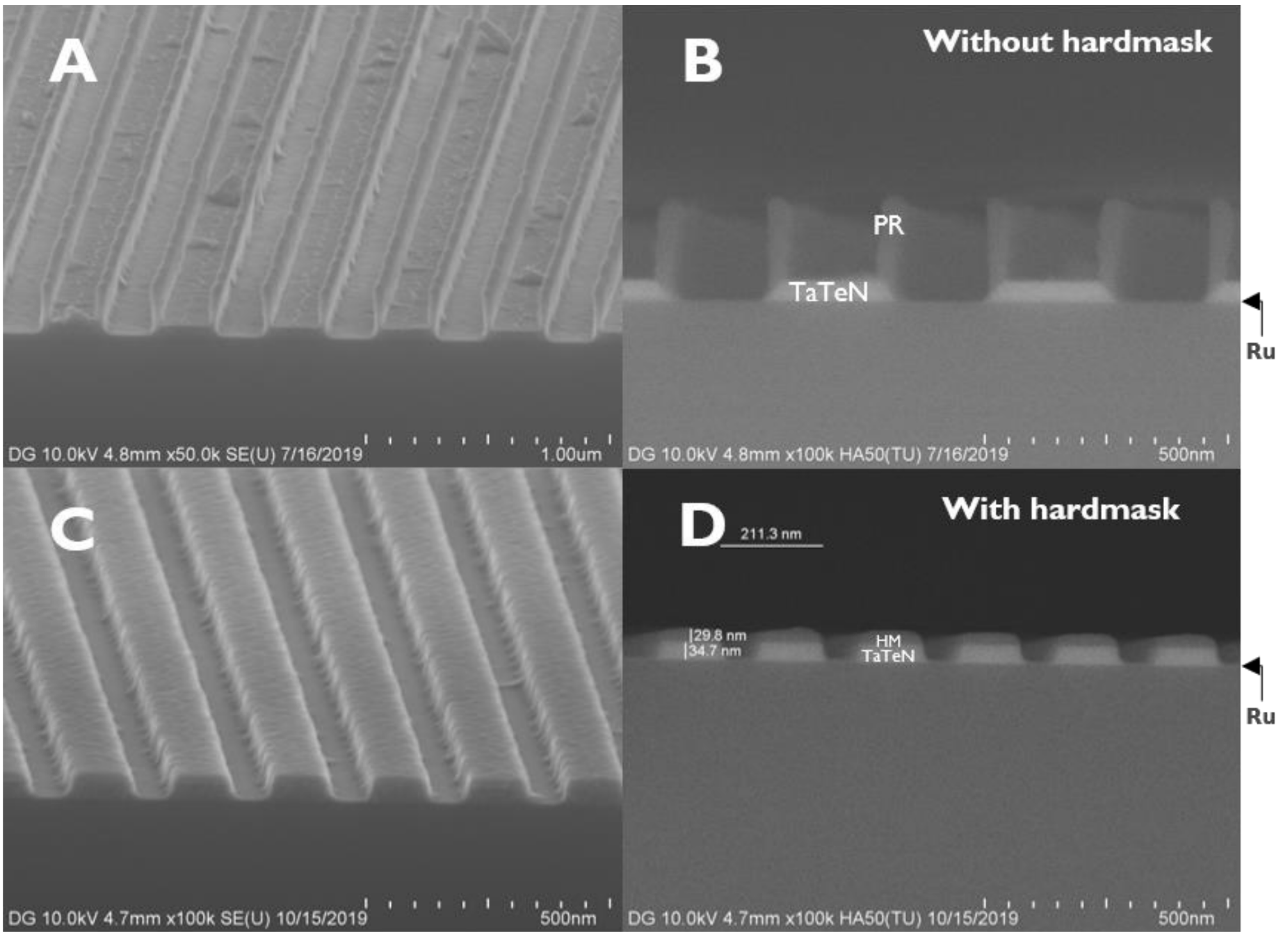

Figure 14. XSEM inspection after TaTeN etching using Cl-based RIE. ***Etch without HM:*** *tilted view (A) and cross section view (B).* ***Etch with HM:*** *tilted view (C) and cross section view (D).*

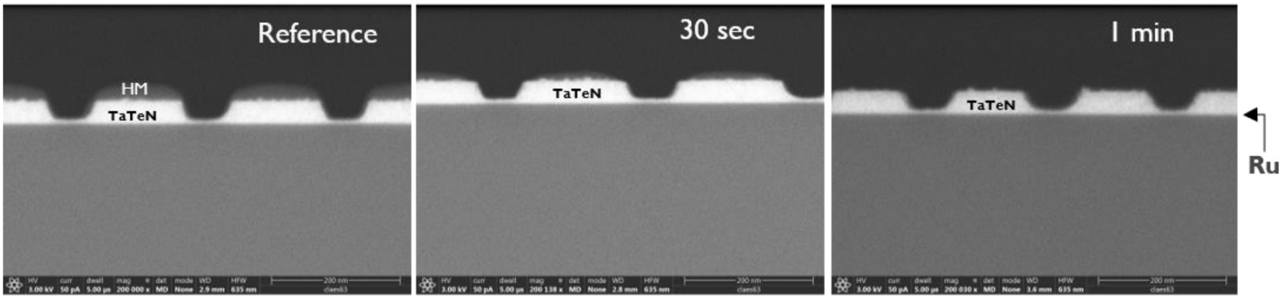

Figure 15. XSEM inspection before and after HM removal by HF dip with different dipping time: 30s and 60s.

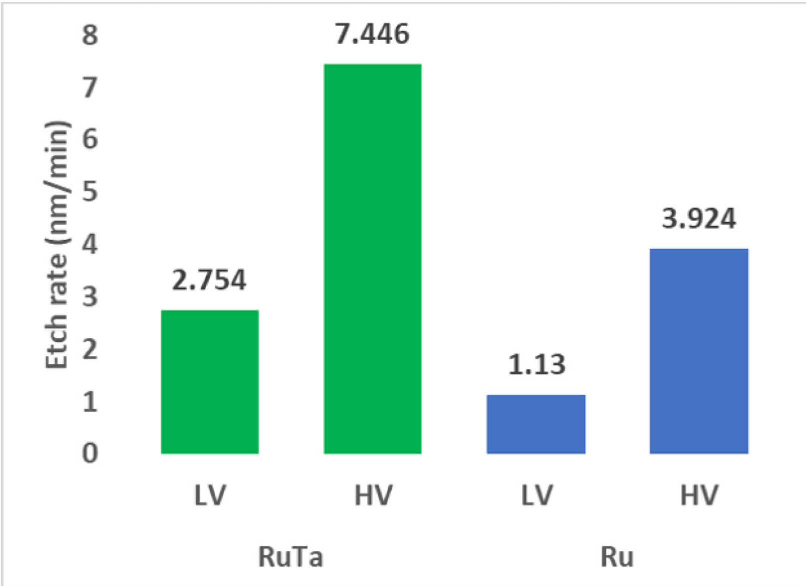

Figure 16. Etch rate of RuTa and Ru using RIE with two recipes: Cl_2 low voltage and Cl_2 high voltage.

[14] A. Erdmann, H. Mesilhy, P. Evanschitzky, V. Philipsen, F. Timmermans, and M. Bauer, "Perspectives and tradeoffs of absorber materials for high NA EUV lithography," *J. Micro/Nanolith. MEMS MOEMS*, vol. 19, no. 04, Oct. 2020, doi: 10.1117/1.JMM.19.4.041001.

[15] M. Wu et al., "Characterization of RuTa alloy as material candidate for EUV attenuated phase shift mask", in preparation.

Industry Briefs

Micron Pulls Ahead on DRAM

By **Gary Hilson,** EETimes

Micron Technology has unveiled its 1-alpha node DRAM, which the company said offers a 40% improvement in memory density over its 1z node DRAM, as well as a 15% improvement in power-savings for mobile devices. This latest memory node supports densities from 8Gb to 16Gb, and Micron has started volume production of DDR4 memory for compute customers and Crucial consumer PC DRAM products on the new process node, while LPDDR4 is being sampled to mobile customers for qualification.

https://www.eetimes.com/micron-pulls-ahead-on-dram/

Major Taiwan Chipmakers to Assign Capacity for Car Use

Focus Taiwan, CNA English News

Taipei, Jan. 27 (CNA) Four major contract chipmakers in Taiwan have agreed to assign capacity to manufacture chips for car use in a bid to alleviate a global shortage of automotive chips, Minister of Economic Affairs Wang Mei-hua (王美花) said, after she met with representatives from the four contract chipmakers — Taiwan Semiconductor Manufacturing Co. (TSMC), United Microelectronics Corp. (UMC), Vanguard International Semiconductor Co. (VIS) and Powerchip Technology Corp. — at a time when global automakers have urged Taiwan to increase automotive chip supplies.

In 2019, automakers cut their orders for chips, prompting local chipmakers to shift their capacity to producing chips for other devices, according to Wang. After the outbreak of the COVID-19 pandemic, demand for notebook computers, smartphones and other devices in a booming global stay-at-home economy further squeezed more of the capacity previously used for car chips. Currently, capacity of the four companies has been almost fully utilized. The urging by global automakers to Taiwan's semiconductor industry for an increase in chip supply indicates that Taiwan plays a key role in the world's economy, the minister said.

The current chip shortage has prompted TSMC and other Taiwanese chipmakers to consider a 15 percent hike in their automotive chip prices which could start in late February.

https://focustaiwan.tw/business/202101270021

China Surges Past Americas and Japan in IC Capacity

Christian G. Dieseldorff, SEMI

Back in 2012, China ranked fifth among seven regions worldwide in IC wafer capacity but surged past the Americas and Japan in 2018 and 2019 to claim the number three position. China's IC wafer capacity growth accelerated to tune of 14% in 2019 and 21% in 2020 and is expected to grow at least 17% this year. But Chinese companies aren't pulling off this feat singlehandedly. Among international-owned companies, TSMC and UMC are driving the largest share of foundry growth, while Samsung, SK Hynix and Intel are powering gains in memory capacity.

https://blog.semi.org/business-markets/china-surges-past-the-americas-and-japan-in-ic-capacity

Join the premier professional organization for mask makers and mask users!

About the BACUS Group

Founded in 1980 by a group of chrome blank users wanting a single voice to interact with suppliers, BACUS has grown to become the largest and most widely known forum for the exchange of technical information of interest to photomask and reticle makers. BACUS joined SPIE in January of 1991 to expand the exchange of information with mask makers around the world.

The group sponsors an informative monthly meeting and newsletter, BACUS News. The BACUS annual Photomask Technology Symposium covers photomask technology, photomask processes, lithography, materials and resists, phase shift masks, inspection and repair, metrology, and quality and manufacturing management.

Individual Membership Benefits include:

- Subscription to BACUS News (monthly)
- Eligibility to hold office on BACUS Steering Committee

spie.org/bacushome

Corporate Membership Benefits include:

- 3-10 Voting Members in the SPIE General Membership, depending on tier level
- Subscription to BACUS News (monthly)
- One online SPIE Journal Subscription
- Listed as a Corporate Member in the BACUS Monthly Newsletter

spie.org/bacushome

CALENDAR

2021

Photomask Japan
20-21 April 2021
Digital Forum
Japan
www.photomask-japan.org

The 36th European Mask and Lithography Conference, EMLC 2021
22 June 2021
Digital Event
www.emlc-conference.com/en

SPIE Photomask Technology + EUV Lithography
26-30 September 2021
https://spie.org/conferences-and-exhibitions/puv

SPIE is the international society for optics and photonics, an educational not-for-profit organization founded in 1955 to advance light-based science and technology. The Society serves more than 255,000 constituents from 183 countries, offering conferences and their published proceedings, continuing education, books, journals, and the SPIE Digital Library in support of interdisciplinary information exchange, professional networking, and patent precedent. In 2019, SPIE provided more than $5 million in community support including scholarships and awards, outreach and advocacy programs, travel grants, public policy, and educational resources. **spie.org**

SPIE.
International Headquarters
P.O. Box 10, Bellingham, WA 98227-0010 USA
Tel: +1 360 676 3290
Fax: +1 360 647 1445
help@spie.org • **spie.org**

Shipping Address
1000 20th St., Bellingham, WA 98225-6705 USA

Managed by SPIE Europe
2 Alexandra Gate, Ffordd Pengam, Cardiff, CF24 2SA, UK
Tel: +44 29 2089 4747
Fax: +44 29 2089 4750
spieeurope@spieeurope.org • **spieeurope.org**

You are invited to submit events of interest for this calendar. Please send to lindad@spie.org.